Design and Analysis of a Novel Traveling Wave Induction Heating System With Magnetic Slot Wedges for Heating Moving Thin Strips

Junhua Wang[1], S. L. Ho[1], W. N. Fu[1], and Y. H. Wang[2]

[1]Department of Electrical Engineering, The Hong Kong Polytechnic University, Hong Kong
[2]Joint Key Lab. of Electromagnetic Fields and Electrical Apparatus Reliability, Hebei University of Technology, Tianjin, China

A novel traveling wave induction heating system with distributed windings and magnetic slot wedges (SW-TWIH) is proposed to address the inhomogeneous eddy-current density problem which dominates the thermal distribution on the surface of work strips. Typical traveling wave induction heating (TWIH) system is replaced by the proposed one enabling the magnetic fluxes generated by each phase to interact and complement with each other and compensate for the weak magnetic areas so as to generate more uniform and concentrated eddy-current density to lead to more homogeneous temperature distribution. In order to realize the performance of the proposed SW-TWIH system and its improved design, finite-element method (FEM) simulations are carried out and reported in this paper. Simulation results of the proposed system are compared with those of a traditional TWIH device and another design, which has distributed windings but without magnetic slot wedges.

***Index Terms*—Eddy current, finite-element method, magnetic slot wedges, traveling wave induction.**

I. Introduction

THE TRAVELING wave induction heating (TWIH) system offers many attractive advantages such as heating uniformity, reliable operation, and high thermal capacity for many applications in the heating and melting industry [1]. It is also commonly used to heat thin steel strips today.

However, there are few reported studies on TWIH when compared to those on longitudinal induction heating systems, even though there are some dedicated analytical studies and numerical methods on transverse flux induction heating (TFIH) systems [2], [3]. Virtually all prior studies introduce some unrealistically over-simplified and impractical assumptions using, for example, a current sheet on a magnetic yoke without slots as the model.

In this paper, a novel traveling wave induction heating system with distributed windings and magnetic slot wedges (SW-TWIH) and its improved system are proposed to address the inhomogeneous eddy-current density that dominates the temperature distribution on the surface of work strip. Magnetic flux distributions and eddy-current distributions are computed using finite-element method (FEM). Performance of the novel SW-TWIH and an improved design is also presented and compared with a typical TWIH [1]–[3] using FEM to showcase the merits of the proposed system.

Similar to the study of traditional longitudinal heaters, two axis equivalent circuit method is usually employed in the steady-state performance study of TWIH [4]. For transient performance, such as eddy-current and temperature field distributions, the results from traditional methods are not as accurate as expected, due to skin effects on the solid pole surface and serious magnetic nonlinearities. With the advent of powerful computing workstations, two-dimensional (2-D) and three-dimensional (3-D) finite-element analyses (FEAs) have now become feasible in practical applications, not only for steady-state field analysis, but also for transient performance study of induction heaters [1], [5]. For complicated TWIHs, transient 3-D FEA study to include the eddy-current and temperature field distributions is, nonetheless, still very computationally expensive and hence are not widely feasible for industrial applications due to its complex 3-D meshing process and excessively long solution time required.

In order to study the performance of the proposed SW-TWIH system, an interpolative FEA modeling method is introduced [6]. The salient performance of the proposed SW-TWIH device can then be obtained accurately using a 2-D transient FEA simulation.

II. Design and Analysis of the Proposed System

Fig. 1(a) is a typical TWIH system and Fig. 1(b) represents the TWIH system with distributed windings but without slot wedges. The proposed SW-TWIH system is shown in Fig. 1(c), which has the same structure with Fig. 1(b) except there are magnetic slot wedges (SW) in each coil. Two linear inductors and thirty three coils are installed on the opposite sides of the strip along the direction of movement to generate the traveling wave. Due to the thickness of the interposing refractory materials, there is a relatively large airgap between the inductor and the strip. For the improved system, a nonmagnetic strip is fitted in the middle of SW as shown in Fig. 1(b). Table I gives the parameters of the proposed system.

For transient analysis, the time step needs to be sufficiently fine, such as 0.01 ms in this study, so as to simulate the eddy-current distribution correctly. Based on the observations, it is estimated that it takes more than a few days to obtain the complete solution with 3-D FEA. Such a long computation period is unrealistic for engineering applications.

Two main causes that contribute to inaccurate simulation results when using 2-D models are the end-turn leakage inductance and the equivalent effective core length and 3-D simulations are indeed necessary to address these issues. It can be shown, however, that 2-D transient FEA model, which uses the

Manuscript received October 31, 2009; revised January 30, 2010; accepted February 06, 2010. Current version published May 19, 2010. Corresponding author: J. Wang (e-mail: junhua.wong@polyu.edu.hk).

Color versions of one or more of the figures in this paper are available online at http://ieeexplore.ieee.org.

Digital Object Identifier 10.1109/TMAG.2010.2043341

TABLE I
DESIGN DATA OF THE PROPOSED HEATERS

The proposed heater	Number of phases	3
	Number of windings	6
	Number of slots	36
	Airgap distance	1.0 mm
	Magnetic yoke length	1400 mm
	Magnetic yoke height	120 mm
	Slot width	33.3 mm
	Slot height	60 mm
Width of aluminum strip		130 mm
Thickness of aluminum strip		3.0 mm
Movement velocity of strip		1.0 m/min
The width of nonmagnetic material in the improved SW-TWIH system		2 mm

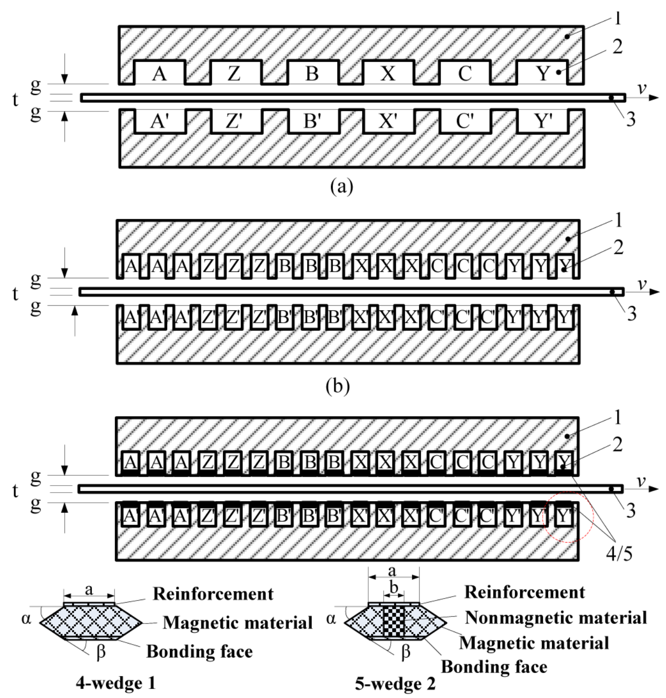

Fig. 1. Schematics of the systems. (1–magnetic yoke; 2–exciting windings; 3–load metal sheet; t-strip thickness; g-airgap between inductor and load; v-strip movement velocity. Initial phase angle: A–X and A'–$X' = 0°$, B–Y and B'–$Y' = -120°$, C–Z and C'–$Z' = -240°$). (a) A typical TWIH with three phases: A–X, B–Y and C–Z. (b) Another TWIH with distributed windings but without slot wedges. (c) SW-TWIH (wedge 1) and improved SW-TWIH (wedge 2).

end-turn leakage inductance and effective core length computed according to the 3-D FEM method described in [6], can be exploited to find a sufficiently accurate solution with realistic computational effort.

III. FEM SIMULATION AND SYSTEM PERFORMANCE

The operation of the novel 3-phase induction heating devices, namely the SW-TWIH system, and its improved system are investigated using FEM. The amplitude of the exciting current is 1200 A at 500 Hz. The winding current phase angles of W1, W2, and W3 are 0°, $-120°$, and $-240°$, respectively, for the equivalent 2-D transient FEA model.

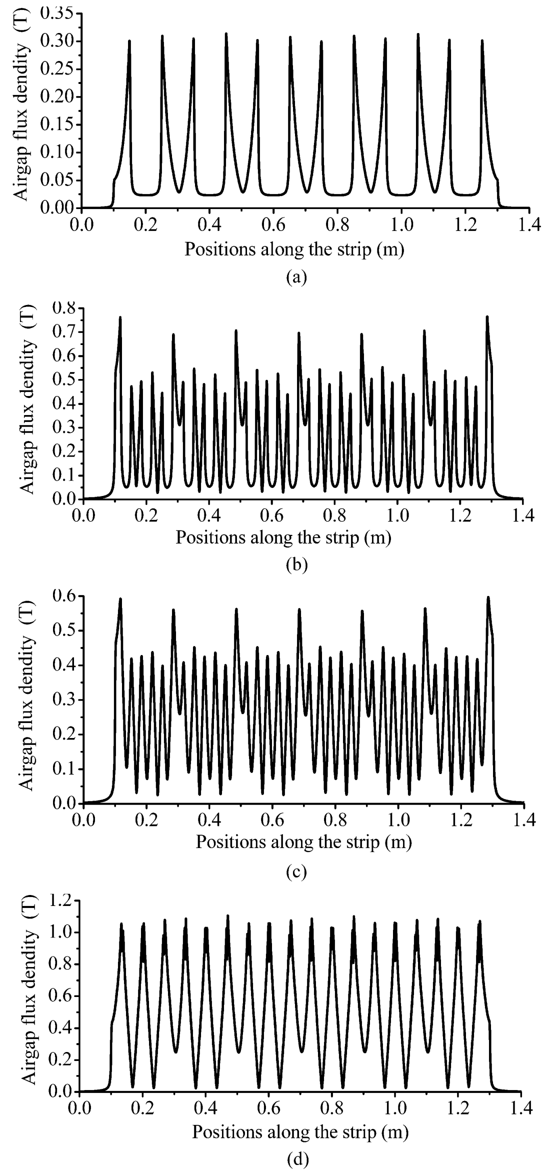

Fig. 2. The airgap flux density distribution along the direction of the strip movement. (a) Typical TWIH system. (b) TWIH system with distributed windings but without slot wedges. (c) Proposed SW-TWIH. (d) Improved SW-TWIH system.

Particular attention is paid to the analysis of the magnetic flux density in the airgap, the eddy-current distribution, and the power density.

A. Analysis of Magnetic Flux Density Distribution

For the magnetic flux density field, the basic equations are established using $\vec{T} - \Omega$ formulation, where $\vec{T}$ is the magnetic vector potential and Ω is the magnetic scalar potential. Applying Ampere's law, Faraday's law, and Gauss's law for the solenoidality of the flux density yields the differential equations in the conducting region as

$$\nabla \times \left(\frac{1}{\sigma}\nabla\times \vec{T}\right) + \frac{d}{dt}(\mu \vec{T} + \mu\nabla\Omega) = -\frac{d}{dt}\left(\mu \vec{H}_S\right) \quad (1)$$

$$\nabla \cdot (\mu \vec{T} + \mu\nabla\Omega) = -\nabla \cdot (\mu \vec{H}_S) \quad (2)$$

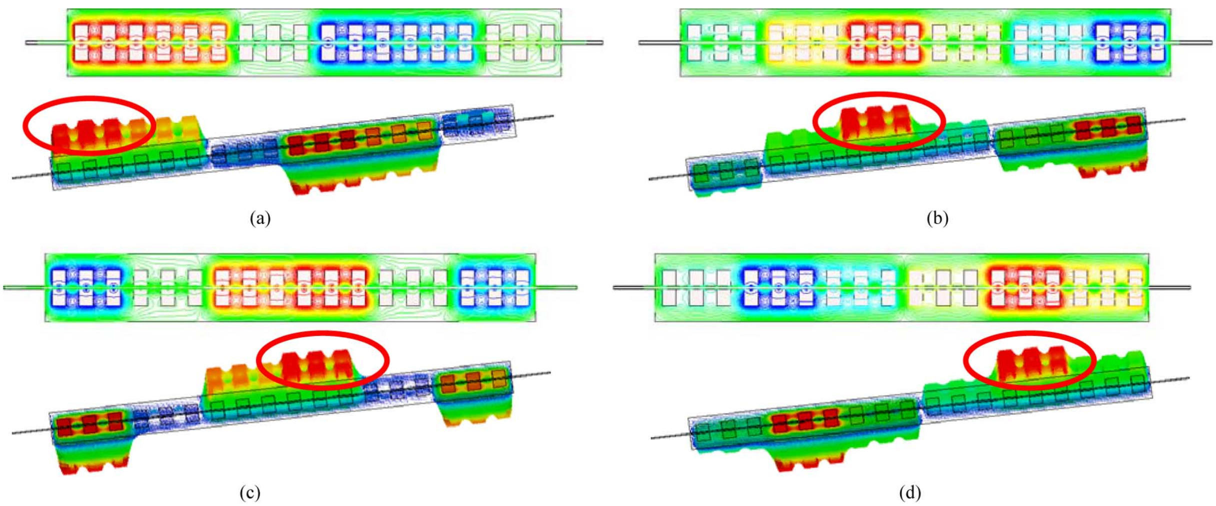

Fig. 3. Magnetic flux distributions of the improved SW-TWIH system along the direction of the strip movement. (The magnetic fluxes as shown in red color and circled are moving from left to right as time increases.) (a) At a phase angle of 0°. (b) At a phase angle of 90°. (c) At a phase angle of 180°. (d) At a phase of 270°.

where $\vec{H}_S$ is a source field, σ is the electric conductivity, and μ is the relative permeability.

Because AC current flowing through every winding generates a magnetic field, which induces eddy currents to produce the thermal field, the total magnetic field is the additive contributions of six pairs of upper-and-lower windings.

Results of the airgap flux densities of the typical TWIH, the TWIH system with distributed windings but without slot wedges, the proposed SW-TWIH and the improved SW-TWIH system are all shown in Fig. 2. In the typical TWIH system, the average trend of the airgap flux density B waveform is symmetrical and has similarly triangular-topped amplitudes and large peaks. With distributed windings but without slot wedges, the airgap flux density becomes larger and more uniform, yet there are still large differences between the flux peaks. For SW-TWIH system and its improved partner, the weak areas of the flux densities between two neighboring coil slots in the inductors are compensated due to the magnetic SW, and the whole flux density distribution becomes more uniform. Compared to SW-TWIH, the improved SW-TWIH system also provides higher flux density because of the nonmagnetic strip in the SW. The curve of the improved SW-TWIH system's magnetic flux density is relatively more homogeneous than those of others, which shows low density only in several limited regions. Thus, the eddy-current field and then the temperature field distributions on the work strip are more uniform in the improved SW-TWIH system when compared with those in other systems mentioned earlier as discussed in Section III-B.

B. Eddy-Current Model Analysis

The relationship between eddy-current density $\vec{J}_S$ and the source field $\vec{H}_S$ is deduced by Maxwell electromagnetic equations as

$$\nabla(\nabla\cdot \vec{H}_S) - \mu\sigma\frac{\partial \vec{H}_S}{\partial t} = \nabla\times \vec{J}_S\,. \tag{3}$$

The induced current density in the strip is generated by variations in the magnetic flux. The vortex effects in the strips are attributed to the magnetic fields produced by different structures of TWIHs or other types of heaters like TFIH devices.

By using FEM, the magnetic flux distributions of the improved SW-TWIH system are shown in Fig. 3 at the phase angles of 0°, 90°, 180°, 270°, and 360°. By focusing on the positive waveform as circled and shown in red color in Fig. 3(a), it can be seen that the positive waveform is moving from the left to the right side of the strip as the phase angle of winding A changes from 0° to 270°. This is where the name 'Traveling Wave Induction Heating' comes from. It also can be seen that the novel improved SW-TWIH system has a relatively more uniform magnetic flux density distribution. This is accomplished mainly because of the application of three-phase AC excitations to create the uniform magnetic fields that govern largely the eddy-current density distribution. On the other hand, the combination of distributed windings and SWs serves to widen the directions of the induced magnetic field which is distributed along the magnetic yokes. These factors interact with each other and compensate for the weak magnetic areas that exist among the various gaps.

Fig. 4 shows the eddy-current density distributions in typical TWIH, the proposed SW-TWIH and the improved SW-TWIH system. It can be seen that the eddy-current distributions are more uniform in the two proposed systems, especially in the improved SW-TWIH, when compared to those in typical TWIH system because of the application of the distributed windings and the magnetic SWs. Also, the combination of six induction heaters serves to widen the directions of the induced magnetic fields along the magnetic yokes. For the improved SW-TWIH system, the nonmagnetic material strip serves to decrease the magnetic flux leakage to result in a relatively higher magnetic flux density.

Another characteristic of typical TWIH system that needs to be considered is the presence of many high eddy-current peaks along the movement directions on the edges of the sheet, which can give rise to, in some cases, dangerous strip deformations. In the proposed SW-TWIH system and its improved partner, this problem is reduced since sharp peaks of eddy currents are much fewer. The eddy-current mean square deviations are 18.7303 for

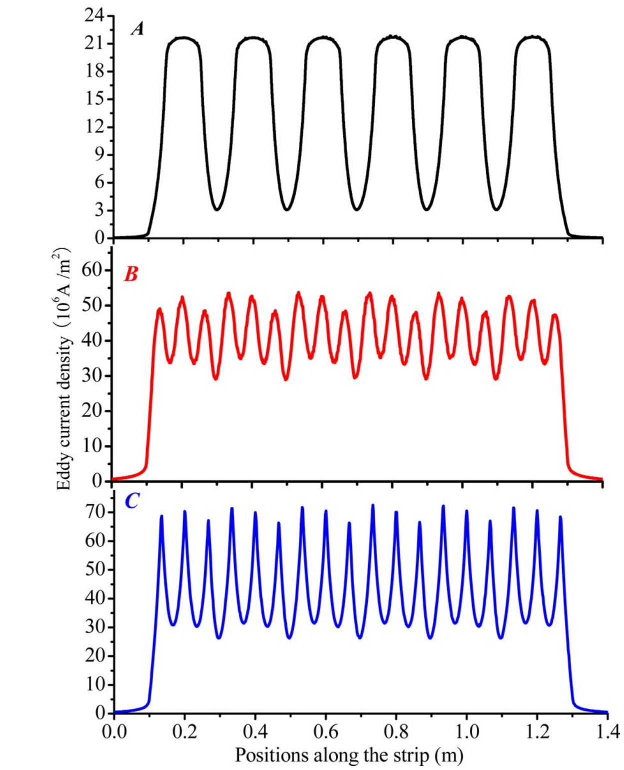

Fig. 4. The eddy-current density distribution in the strip: (a) typical TWIH, (b) SW-TWIH, and (c) improved SW-TWIH.

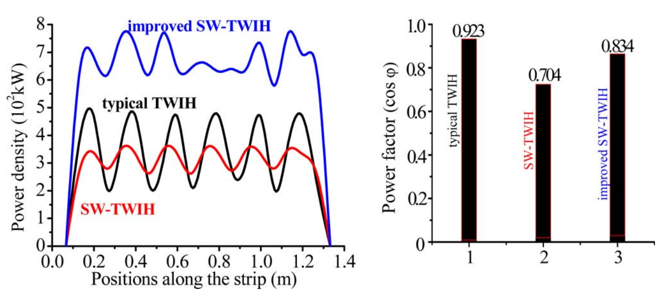

Fig. 5. Relative power density distributions and the power factor.

the typical TWIH being studied, 8.606 for the SW-TWIH and 11.731 for the improved SW-TWIH, respectively.

The best cases among the typical TWIH, the proposed SW-TWIH and the improved SW-TWIH system are compared in Fig. 5, where the irregularities due to the use of a relatively small number of mesh elements have been smoothened. It can be seen that from 0.16 m to 1.32 m, the SW-TWIH and improved SW-TWIH systems, particularly the latter, produce more uniform power density than that in the typical TWIH system being studied. The improved SW-TWIH system also attains nearly double power density distributions comparing to the other two systems. Hence, the improved SW-TWIH system provides relatively more homogeneous power distributions and much larger power supply. The power factor of 0.834 of the

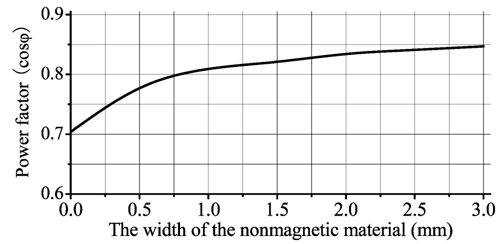

Fig. 6. The power factor with different widths of nonmagnetic material.

improved SW-TWIH also compares favorably with 0.704 of the SW-TWIH.

For the improved SW-TWIH, the power factor changes with the airgap width of the nonmagnetic material in the magnetic slot wedges, and Fig. 6 shows the trend. The power factor becomes higher when the width of the nonmagnetic material is increased, but the distribution uniformity becomes worse according to our numerical analysis. Hence, it is essential to select a compromise value based on practical requirements in order to balance uniformity and power factor.

IV. Conclusion

In this paper, a novel traveling wave induction heating system with distributed windings and magnetic slot wedges, namely SW-TWIH and the improved one, for the continuous heating of thin metal sheets have been analyzed. The performances of the improved SW-TWIH system compares very favorably with those of typical TWIH system. Distributions of magnetic flux, eddy-current density and power density along the position of the strip are studied and improved by applying different types and dispositions of yokes and coils. The good performance of the proposed system, especially the improved one, has been verified by using FEM simulation.

Acknowledgment

This work was supported by the National Natural Science Foundation of China under Grant 50877022.

References

[1] S. L. Ho, J. H. Wang, W. N. Fu, and Y. H. Wang, "A novel crossed traveling wave induction heating system and finite element analysis of eddy current and temperature distributions," *IEEE Trans. Magn.*, vol. 45, no. 10, pp. 4777–4780, 2009.
[2] N. Bianchi and F. Dughiero, "Optimal design techniques applied to transverse-flux induction heating systems," *IEEE Trans. Magn.*, vol. 31, no. 3, pp. 1992–1995, 1995.
[3] Z. M. Wang *et al.*, "Eddy current and temperature field computation in transverse flux induction heating equipment," *IEEE Trans. Magn.*, vol. 37, no. 5, pp. 3437–3439, 2001.
[4] A. L. Bowden and E. J. Davies, "Travelling wave induction heaters design considerations," in *BNCE-UIE Electroheat for Metals Conf.*, Cambridge, U.K., Sep. 21–23, 1982.
[5] S. Lupi *et al.*, "Comparison of edge-effects of transverse flux and travelling wave induction heating inductors," *IEEE Trans. Magn.*, vol. 35, no. 5, pp. 3556–3558, 1999.
[6] Y. B. Li, S. L. Ho, W. N. Fu, and W. Y. Liu, "An interpolative finite-element modeling and the starting process simulation of a large solid pole synchronous machine," *IEEE Trans. Magn.*, vol. 45, no. 10, pp. 4605–4608, 2009.